Modelling and optimisation of continuous clarifier operations from batch jar test data

SH Barthelme
Elphin Lodge, PO Box 891039, Lyndhurst 2106, South Africa

Abstract

The conventional laboratory jar testing procedure which is utilised in the design and process description of the rapid mix and flocculation processes of water clarification may be adapted to describe the operation of a full-scale continuous shallow depth sedimentation unit process. It was found that in analysing the flocculation kinetics of the jar test, the floc break-up rate and floc aggregation rate constants are statistically correlated to the floc settling velocities. The constants in the correlation are typical for the particular type of water and provide a link between the batch jar test and the continuous sedimentation process.

The laboratory jar test is also useful in evaluating the effect of clarifier hydraulic characteristics, such as short circuiting and back mixing. Such a study done on a lamella settler showed that the clarifier will not perform satisfactorily without a flocculation basin preceding the plate pack, since the velocity gradients are low and of too short a duration. The jar test may also be used to optimise a clarifier configuration instead of resorting to pilot-plant studies.

Introduction

The mechanism for the removal of colloidal particles in suspension in water has been extensively researched and modelled around the coagulation, flocculation and sedimentation unit processes. Coagulation involves the neutralising of electrical charges on the particles, which for clay particles result from imperfections in the crystal lattice structure. Metal salts such as $Al_2(SO_4)_3$ and $Fe_2(SO_4)_3$ are used to neutralise these charges. Typical relationships between residual turbidity, colloid concentration and coagulant dose for the coagulation process have been presented by Benefield et al. (1982). Once the optimum coagulant dosage, pH and rapid mix conditions have been established, the water is transferred to a flocculation tank in which gentle agitation produces particle contact between destabilised colloids, so that larger aggregates can form which are large enough to be removed by sedimentation.

Different waters, however, have different treatment requirements and what the design engineer requires is a relatively simple tool around which he can model the coagulation, flocculation and sedimentation unit processes. This model should ideally incorporate all design variables which need to be considered in practice. The most widely used method in evaluating the coagulation-floccuation processes to date is the laboratory jar test. Hudson (1981) has presented an in-depth summary of the variables involved and the equipment needed to run the jar test to obtain meaningful results.

Argaman and Kaufman (1970) have presented a model for turbulent flocculation comprising 2 components, namely the floc aggregation and floc break-up rate of primary particles (or turbidity). The effectiveness of the removal of primary particles or colloids by their conversion into flocs for a system consisting of *i* completely mixed flocculator compartments in series of equal volume with a total residence time of T was given as:

$$\frac{n_0}{n_i} = \frac{\left(1 + k_A GT/i\right)^i}{1 + k_B G^2\, T/i \left[\sum_{m=0}^{i-1} \left(1 + k_A GT/i \right)^m \right]} \quad (1)$$

Received 15 January 1993; accepted in revised form 12 August 1993.

where:

- n_o - initial concentration of primary particles (or turbidity) at time t = 0
- n_i - concentration of primary particles (or residual turbidity) after flocculation for a time t = T followed by "infinite" settling
- k_A - floc aggregation rate constant
- k_B - floc break-up rate constant (s)
- G - root mean square velocity gradient (s^{-1})

Bratby et al. (1977) showed that the constants k_A and k_B remain the same for a batch jar test and for a continuous flow operation. The equivalent flocculation equation for a batch system is given as:

$$\frac{n_0}{n_1} = \left[\frac{k_B}{k_A} G + \left[1 - \frac{k_B}{k_A} G \right] e^{-k_A GT} \right]^{-1} \quad (2)$$

Argaman (1971) has shown that k_A and k_B are the same for small and large-scale plants treating the same effluent. Therefore Eqs. 1 and 2 may be used to obtain a first estimate in the laboratory of parameters affecting the design of flocculation basins. The constants k_A and k_B have also been shown to be characteristic of a specific water (Janssens and Beukens, 1987) and need to be evaluated every time a different water is treated.

The information obtained from performing a series of jar tests has, however, been limited to the upscaling of the coagulation and flocculation unit processes. What is required is an idea of whether the laboratory jar test is of any use in the design and optimisation of the sedimentation tank which follows the flocculation basin. The direct scale-up of settling data from the jar test to a conventional settling basin is viewed with some scepticism since the settling depth in the jar is much less than that of a full-scale plant. This usually results in large plants producing superior effluent qualities since additional flocculation takes place as flocs settle through the greater vertical settling distance, entrapping smaller particles in their passage to the tank bottom. This is commonly known as "sweep" or vertical flocculation.

In Eqs. 1 and 2, n_i is taken as the residual turbidity measured

after an "infinite" settling time in the jar. "Infinite" settling is defined as the time when no further reduction in residual turbidity with an increase in settling time can be measured of the flocculated water (normally taken as 45 min). "Infinite" settling does not, however, provide an estimate of the settling velocity of the flocs and is not necessarily duplicated in the full-scale plant.

Evidently there are many variables which may influence the clarification process. It is for this reason that pilot plants are sometimes built in addition to jar testing which simulate the conditions envisaged in the full-scale operation. Pilot plants are, however, costly and geometrical configuration changes often impossible because of the inflexibility of the design. To optimise the clarifier from a pilot plant may, therefore, be economically prohibitive. It would be more convenient if the jar test model could be used for this purpose.

A project was undertaken to model a package lamella clarifier around the jar test to investigate any correlations that might exist between the laboratory jar test, used in conjunction as a column test, and the continuous operation. The influence of the lamella clarifier's residence time characteristics, plate flocculation and the optimisation of the clarification process from the laboratory jar test were investigated.

Apparatus

Clarifier

The clarifier was a type of lamella settler in which the sedimentation region consisted of one truncated cone stacked on top of the other, with the flocculation basin positioned on top of the plate pack (Fig. 1). The coagulation basin was located within the flocculation basin. Hence the 3 unit processes where housed within the same holding tank. The conical plates were constructed out of glass-reinforced fibre and have gutters moulded into them which assist in channelling the sludge from the inclined plate surface directly to the bottom desludging valve. The angle of inclination of the plates was $\alpha = 56{,}6°$ and the sludge gutters had an angle of 60° to the horizontal. The gutter arrangement prevents the resuspension of settled flocs into the influent as particles fall past consecutive plate spacings lower down. For the other physical dimensions of the conical plates and the holding tank, see Table 1.

The flocculation basin was agitated by a 45° pitch axial flow impeller driven by a DC motor whose speed was controlled by a potential divider to allow stepless rotational speeds ranging from $N = 0\ r{\cdot}min^{-1}$ to $N = 50\ r{\cdot}min^{-1}$. The rapid mix reactor was located

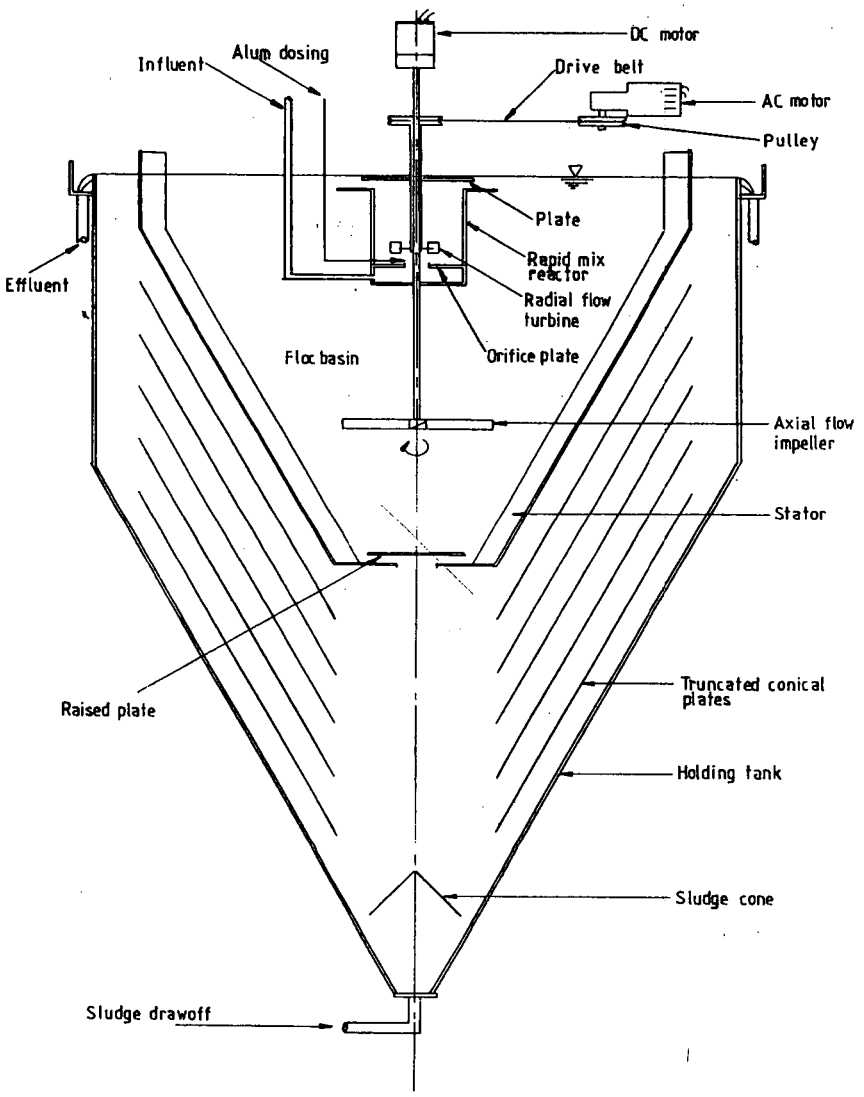

Figure 1
The conical lamella settler

TABLE 1 PHYSICAL DIMENSIONS OF THE CONICAL PLATES AND THE HOLDING TANK	
Parameter	**Value**
Angle of cone inclination (α)	56,6°
Angle of sludge gutter inclination	60°
Outer cone truncation radius (H)	0,43 m
Inner cone truncation radius (h)	0,155 m
Plate spacing (Z)	0,04 m
Diameter of holding tank	0,985 m
Cylindrical height of holding tank	1,04 m
Flocculation basin diameter	0,855 m
Number of plate spacings (n)	9

centrally within the flocculation basin and its contents was mixed using a radial flow turbine. The axial flow impeller shaft rotated within the radial flow turbine shaft. The turbine was driven independently by an AC motor with a pulley system. The speed of the motor was controlled by a variac. Coagulant was dosed into the rapid mix unit via a constant head tank into the eye of the turbine. Impeller rotational speeds were measured with photo-electric probes.

Figure 2 shows the pipe network used to operate the clarifier. The reservoir which contained the effluent to be treated was continuously agitated in order to ensure a uniform influent concentration. It was also equipped with heating elements which maintained the temperature of the water at 25°C ± 1°C.

Steady state conditions in the operation of the clarifier were easily achieved, since the reservoir had a capacity of 14,5 times the flocculation basin hydraulic retention time and 6,3 times the sedimentation zone retention time. Tracer tests done on the clarifier also confirmed that the system reached greater than 99% of the equilibrium state before the reservoir's capacity was exhausted.

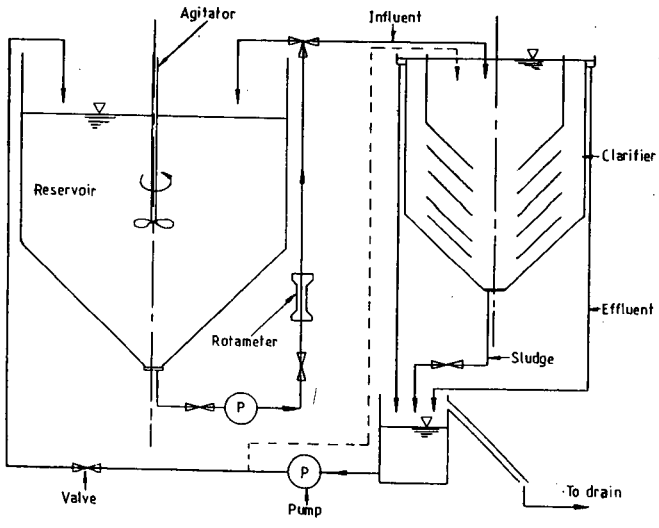

Figure 2
Pipe network

Jar test apparatus

The jar test apparatus was constructed in such a manner as to model the clarifier on a small scale in as many ways as possible. Bratby et al. (1977) have shown that the geometry of the flocculation reactor has a considerable influence on the performance of the reactor and hence the final effluent clarity. Therefore, for the jar test to simulate as closely as possible the conditions in the clarifier, the circular cross-section of the flocculation basin in the lamella clarifier is represented by a cylindrical jar. The jar was constructed from perspex with its depth equal to its diameter (142 mm) and a volumetric capacity of V = 2,297 *l*. A sampling tap was installed on the side of the jar from which the water samples were withdrawn. The depth of the sampling tap below the surface water level was 75 mm. This depth is of the same order as the vertical settling distance that a particle traverses between parallel plates of a lamella clarifier inclined at 56° to the horizontal and spaced 40 mm apart. Other features duplicated geometrically from the flocculation basin and coagulation reactor to the jar were the 4 stator baffles and the stirrers used for agitation.

Impellers and root mean square velocity gradients

Lai et al. (1975) among others have shown how a jar with a certain impeller configuration can be calibrated to yield values of the root mean square velocity gradient G for different stirrer rotational speeds. Camp and Stein (1943) defined G as follows:

$$G = \sqrt{\frac{P}{V\mu}} \qquad (3)$$

where:

- G - Root mean square velocity gradient (s^{-1})
- P - Power input into the liquid of the mixing chamber (w)
- μ - Absolute viscosity ($kg \cdot ms^{-1}$).

Although the G value is viewed with scepticism as to its validity in designing flocculation and rapid mix basins (Cleasby, 1984), from an operational point of view G can, to a satisfactory degree, describe the observed data, and it is for this reason that it is still widely used in design. The power imparted to the liquid with the impeller is best determined through measurements of the torque on the agitator shaft at various rotational speeds. For the jar, torque measurements for the axial flow flocculation impeller were performed by suspending the jar from the ceiling on a length of fishing gut (Fig. 3). When the impeller rotated within the freely suspended jar, the viscous shear set up by the agitator caused the jar to twist about its centre. The jar was then brought back to its original position by placing a small weight on a dish which was connected to the outer diameter of the jar with a light cotton thread. The cotton thread ran around a small bearing and the system was brought to equilibrium by adjusting the agitator rotational speed on a potential divider to the value that kept the jar stationary for a particular mass on the dish. The torque, and hence the power, were computed as follows:

To = force x lever arm
To = Mg x lever arm

$$P = \frac{2\pi N\,To}{60} \qquad (4)$$

where:

- M - mass of weight on dish (kg)
- To - torque (N·m)

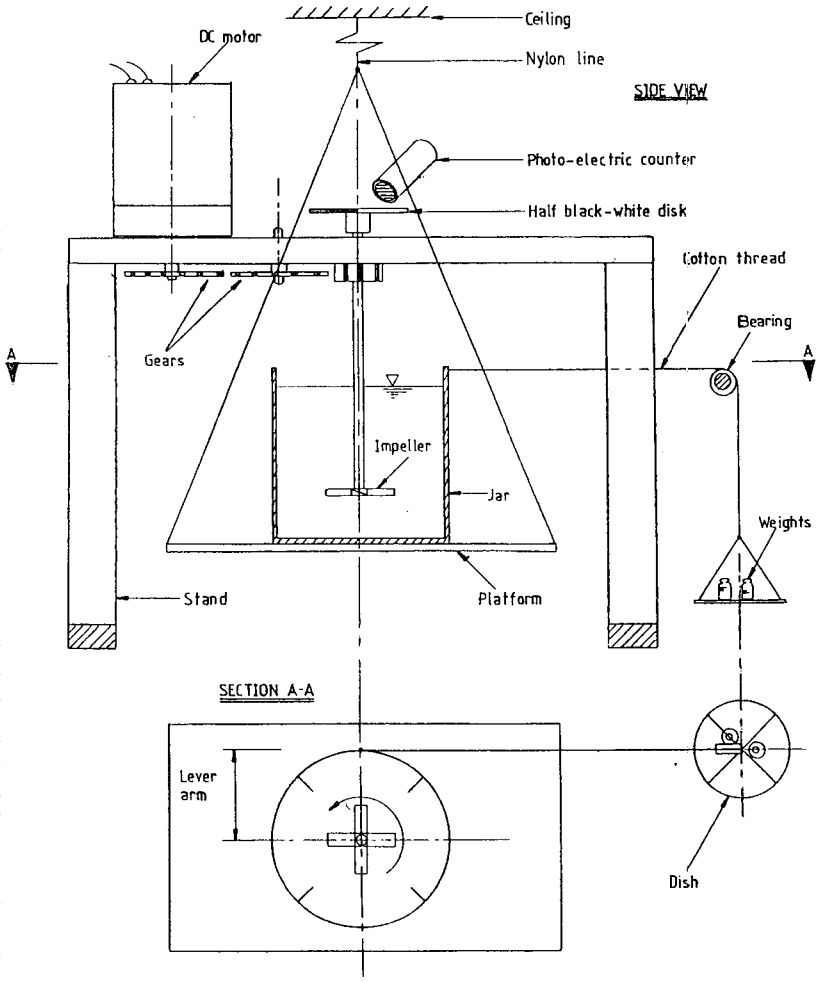

Figure 3
Schematic representation of jar calibration apparatus

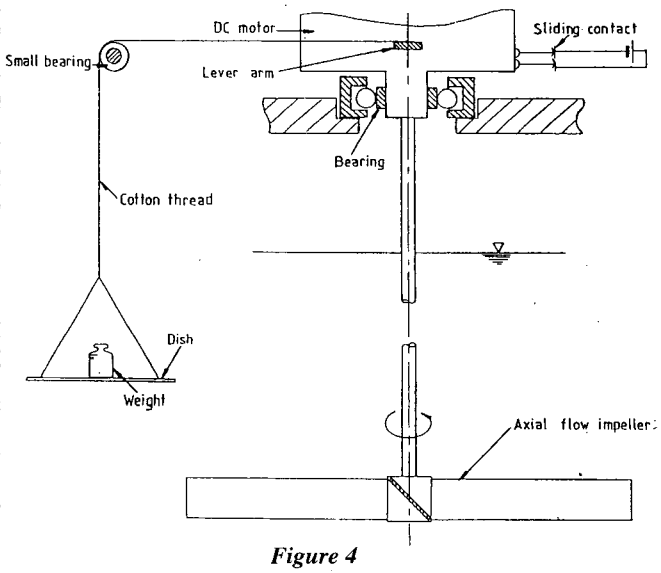

Figure 4
Dynamometer arrangement for torque measurement of the flocculation basin impeller

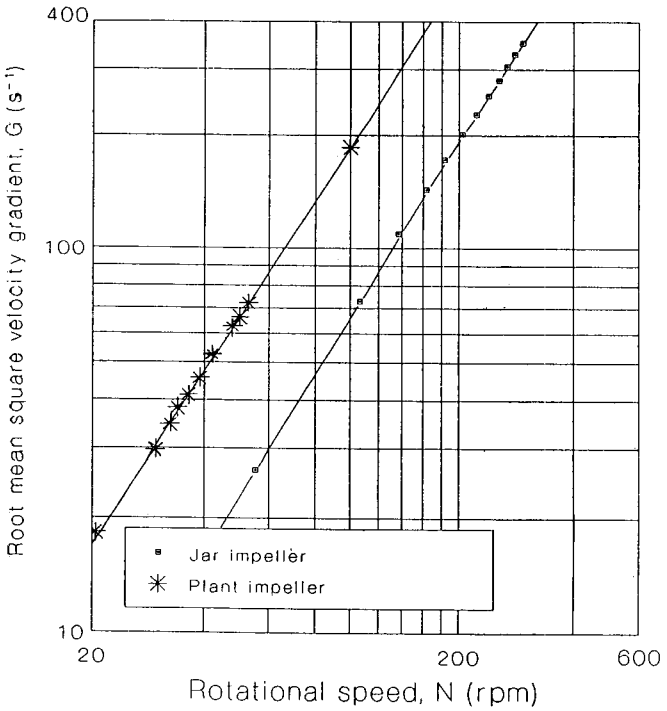

Figure 5
Impeller calibration curves

g - gravitational constant ($m \cdot s^{-2}$)
P - power input into the liquid (w)
N - rotational speed of impeller ($r \cdot min^{-1}$)

The calibration of the flocculation basin axial flow impeller in the lamella clarifier was done using a similar dynamometer arrangement for torque measurement (Fig. 4). Here the DC motor was brought to rest by adjusting the impeller rotational speed. Geometric scale-up of the axial flow flocculation impeller from the jar to the clarifier was based on the ratio of the impeller to tank diameter and the proximity of the impeller to the tank bottom (Bates et al., 1963). The calibration curves for the jar and clarifier flocculation impellers are given in Fig. 5.

For the purpose of rapid mixing, a high shear rate radial flow turbine was used in both the laboratory jar tests as well as the clarifier rapid mix reactor. The clarifier rapid mix reactor had the same diameter as the laboratory jar. A separate stand was constructed upon which an AC motor was mounted whose speed could be changed with a variac in stepless increments from 200 $r \cdot min^{-1}$ to 750 $r \cdot min^{-1}$. The same radial flow turbine was used in both the laboratory jar and the clarifier rapid mix reactor. A 2 s rapid mix time was chosen for both jar and clarifier. The hydraulic retention time of the rapid mix reactor in the clarifier was kept constant at 2 s as successively higher or lower flow rates were introduced, by raising or lowering a sleeve around the reactor which changed its volume accordingly.

The radial flow turbine was designed as a "standard" 6-flat blade turbine whose power number P_o is equal to 5 in the turbulent mixing range (Leentvaar, 1980). The dimensionless power number is given by:

$$P_o = P/N^3D^5\rho \quad (5)$$

where:
P_o - dimensionless power number
N - rotational speed ($r \cdot s^{-1}$)
D - turbine diameter (m)
ρ - fluid density ($kg \cdot m^{-3}$)
P - power input into the liquid (w)

A G value of 1 000 $\cdot s^{-1}$ was used for rapid mixing, both in the jar and the clarifier. Solving Eqs. 3 and 5 for a turbine diameter of D = 0,0477 m results in a rotational speed of 711 $r \cdot min^{-1}$ for rapid mixing.

In both the clarifier and the laboratory jar test, coagulant was injected into the eye of the radial flow rapid mix turbine to effect optimal mixing. In the above manner, variables affecting rapid mixing were kept constant in both the jar test and clarifier for all retention times. In this way, rapid mixing was excluded as a variable in the model analyses.

Raw waters and jar test procedure

Jar tests and clarifier runs were conducted on 2 different types of colloidal suspensions. Bentonite and kaolin clays were mixed with tap water to produce the following 2 test effluents and their respective alum coagulating concentrations (see Table 2).

Jar tests were conducted by filling the jar to the pre-determined level with raw water, placing the stand with the rapid mix turbine in the jar and injecting alum into the eye of the rotating impeller with a syringe. After 2 s, the rapid mix turbine stand was removed and replaced with the axial flow flocculating impeller stand. The axial flow impeller rotational speed was pre-set to give the desired root mean square velocity gradients which were varied between G = 10 $\cdot s^{-1}$ and G = 60 $\cdot s^{-1}$. Flocculation periods ranged from T= 0 min to T= 30 min. In all instances, a significant horizontal portion of the graph of residual turbidity versus flocculation time was produced, i.e. no further reduction in residual turbidity for a specified settling time with an increase in flocculation time was achieved. Samples withdrawn from the jar were analysed for residual turbidity using a HACH 2100A turbidimeter.

TABLE 2
TEST EFFLUENTS AND THEIR RESPECTIVE ALUM COAGULATING CONCENTRATIONS

Parameter	Bentonite suspension	Kaolin suspension
Initial turbidity (ntu)	40	40
Clay concentration ($mg \cdot t^{-1}$)	152	100
Initial pH	7,9	8,1
Alum dose ($mg \cdot t^{-1}$)	70	20
Alum dilution with distilled water (%)	1,25	0,36
Final pH	6,7	7,6
Temperature (°C)	25	25
Initial alkalinity ($mg \cdot t^{-1}$ as $CaCO_3$)	74	74

Analysis of jar test results

The flocculation efficiency factor n_o/n_1 of Eq. 2 is only applicable to subsequent clarifiers in which so-called "infinite" settling has taken place. Lamella settlers are, however, characterised by their short retention times (usually in the range of 10 to 20 min) and it is therefore impossible to expect Eq. 2 to provide a reasonable estimate of n_1, or conversely to operate the clarifier at such a low overflow rate in order to achieve a 45 min "infinite" retention time in the sedimentation region. Hence samples were withdrawn from the jar at times other than the "infinite" settling time (between 3 and 45 min). Modelling each settling curve individually around Eq. 2 requires a different set of flocculation rate constants. The distinct minimums in the residual turbidity vs. flocculation time relationships obtained from some of the jar tests were extended asymptotically from the minimum as proposed by Andreu-Villegas and Letterman (1976). Curves of flocculation efficiency vs. flocculation time for the kaolin suspension are given in Fig. 6. If the floc aggregation rate constants k_A and the floc break-up rate constant k_B so obtained from the jar tests are plotted vs. the overflow rate v_s corresponding to a specific jar settling time, a good correlation is obtained on a log-log plot for k_B (Fig. 7) and a linear relationship for k_A (Fig. 8).

The best-fit equations to the curves for the kaolin and bentonite suspensions are given in Table 3.

TABLE 3

Raw water	k_A versus v_s	k_B versus v_s
Kaolin	$k_A = (3,65\ v_s + 2,14) \times 10^{-5}$	$\log(k_B) = 1,2712 \log v_s - 6,6028$
Bentonite	$k_A = (-8,226\ v_s + 7,062) \times 10^{-4}$	$\log(k_B) = 1,72 \log v_s - 5,5303$

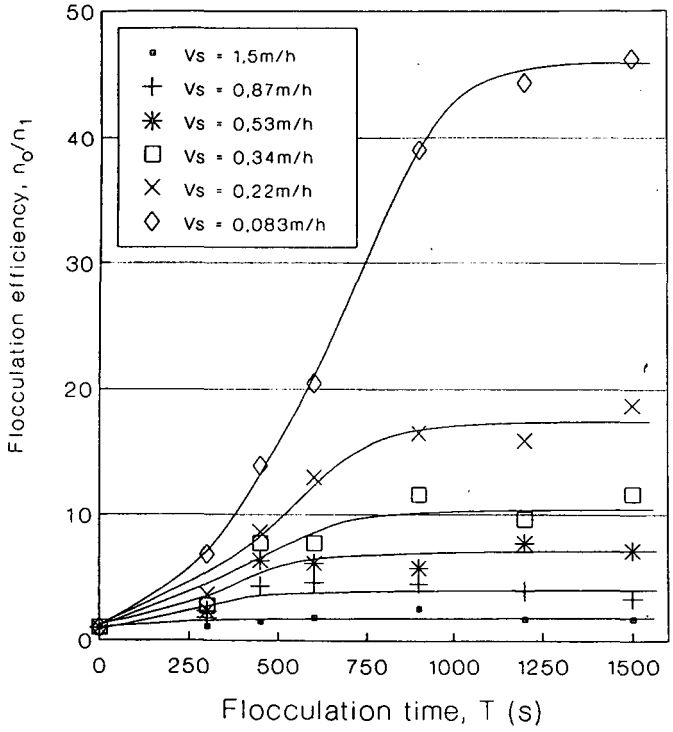

Figure 6
Jar test results obtained by flocculating the kaolin suspension at G = 33,3·s^{-1}.

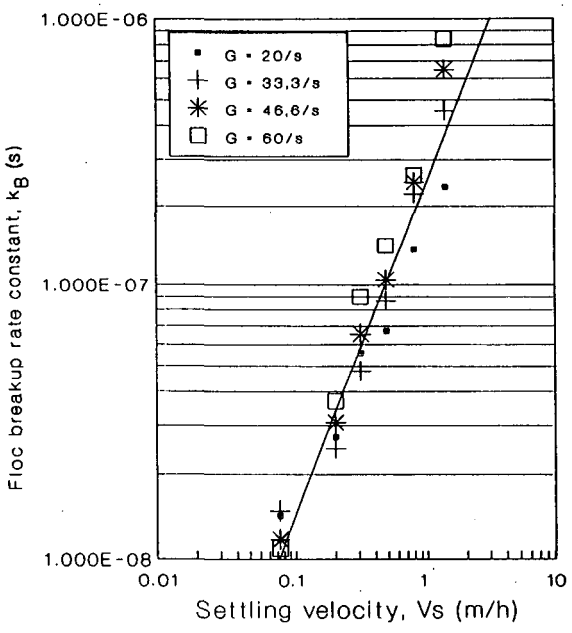

Figure 7
Floc break-up rate constant vs. jar settling velocity for the kaolin suspension

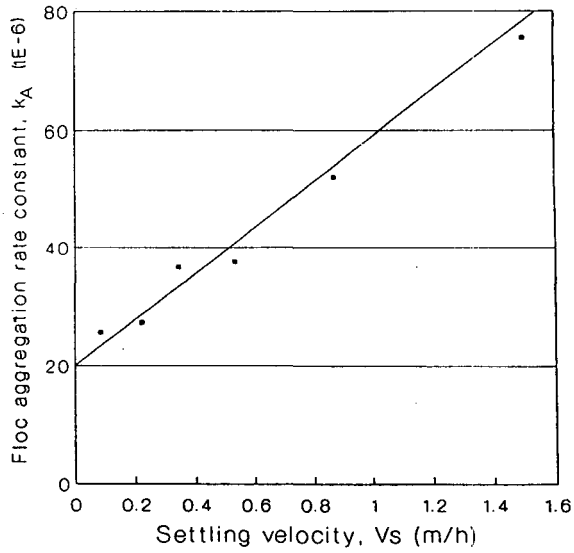

Figure 8
Floc aggregation rate constant vs. jar settling velocity for the kaolin suspension

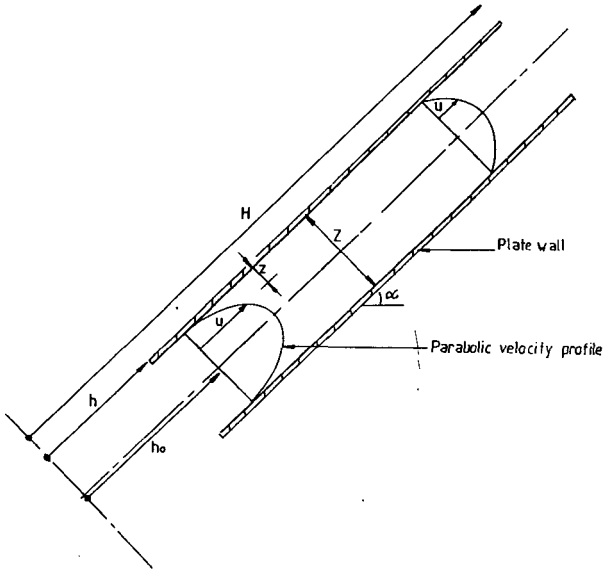

Figure 9
Laminar flow velocity profiles between conical plates

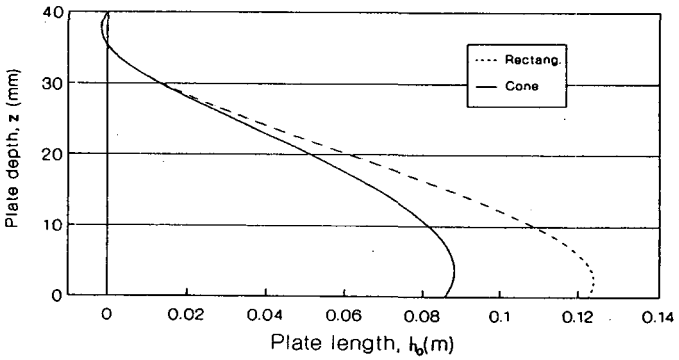

Figure 10
Comparison of a rectangular and conical plate settler particle trajectory

The above correlations show that a water's flocculation characteristics may be described in terms of relationships involving the overflow rate v_s ($m \cdot h^{-1}$) and empirical constants which are typical for the particular water. If the equations in Table 3 are substituted into Eq. 1 and the root mean square velocity gradients G imparted by the impellers in the flocculation compartments of hydraulic retention time T are substituted, a model exists which could predict the performance of a continuous flow clarifier subject to various overflow rates v_s. What is needed is an estimate of the overflow rate v_s for the clarifier in question which is a function of its geometry and total flow rate passing through it.

Yao (1970) has presented a methodology of obtaining the overflow rate for rectangular plate settlers. Particle trajectories are calculated from the entrance to the plate pack to the lower surface which determines the length of plate required to settle out a particle with a certain discreet velocity v_s. For truncated conical plates, however, the laminar velocity profile set up between the parallel plates flattens out with an increase in cone radius as shown in Fig. 9.

This results in particles settling out sooner along the conical plate length as opposed to the rectangular plate. Barthelme (1989) has shown that the trajectory, and hence the overflow rate of truncated conical plates, is described by:

$$v_s = \frac{3Q}{\pi Zn(\cos^2\alpha)h_o}\left[\frac{dz}{dh_o}\left[\frac{z}{Z} - \left[\frac{z}{Z}\right]^2\right]\right] - \frac{dz}{dh_o}\tan\alpha \quad (6)$$

where:

- Q - total flow rate through lamella settler ($m^3 \cdot h^{-1}$)
- n - number of plate spacings
- Z - plate spacing (m)
- z - perpendicular distance from plate surface such that $0 < z < Z$ (m)
- α - angle of inclination of the cones
- h_o - cone radius such that $h < h_o < H$ (m)

In Eq. 6 the variables are neither separable nor is the equation homogeneous and it is therefore solved numerically. Figure 10 shows a solution of Eq. 6 and a corresponding rectangular plate settler particle trajectory for the same variables.

When Eq. 6 is substituted into Eq. 1 and all the relevant values

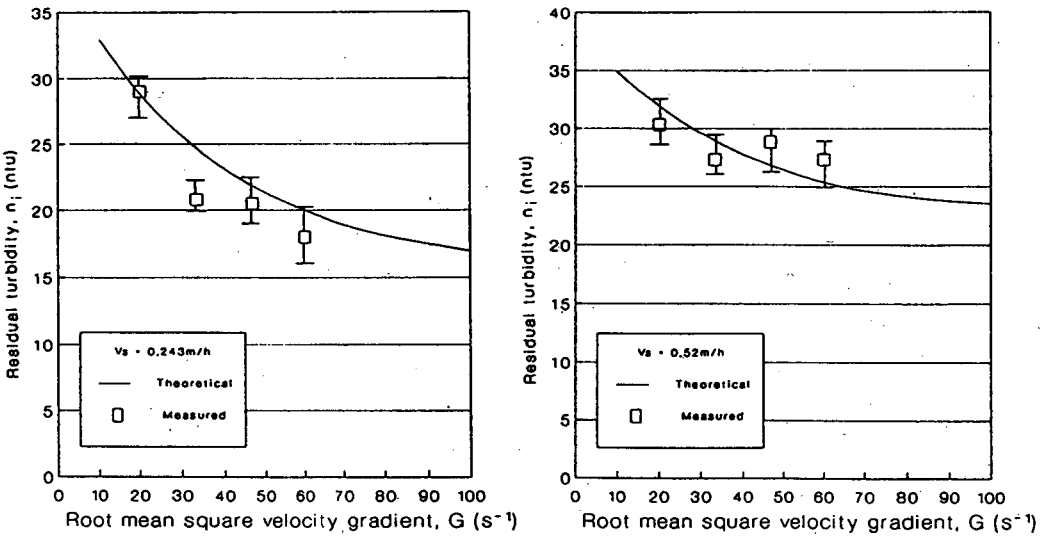

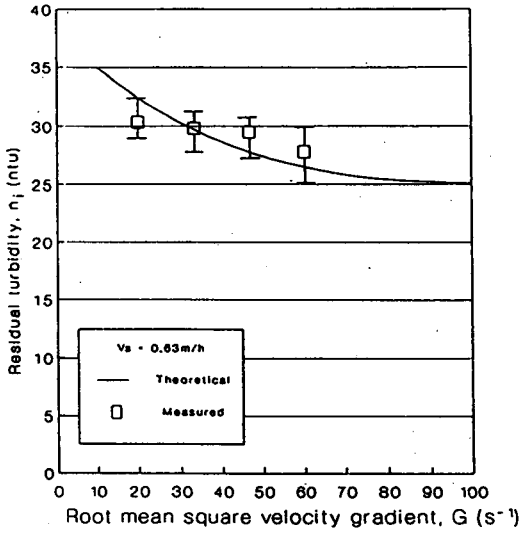

Figure 11
Theoretical and measured clarifier performance for the kaolin suspension

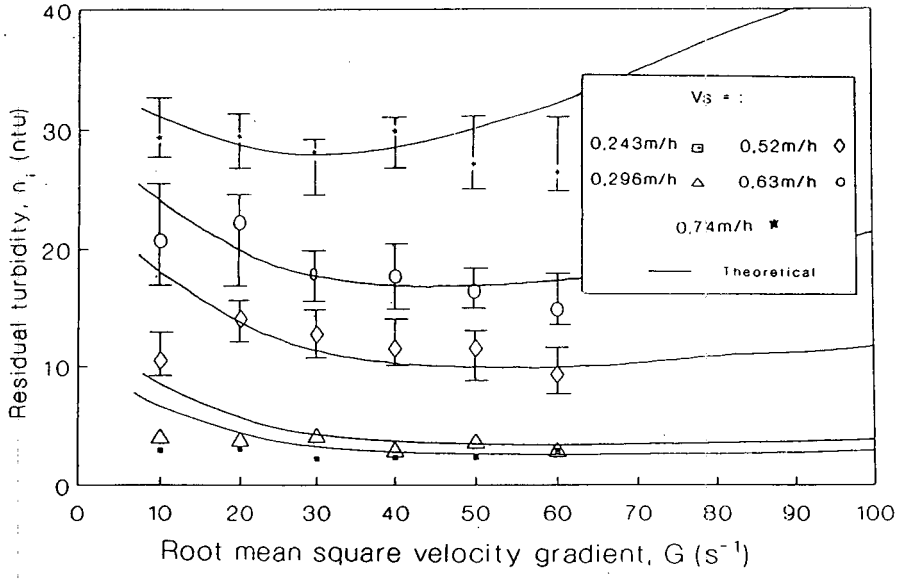

Figure 12
Theoretical and measured clarifier performance for the bentonite suspension

are substituted, the turbidity (n_t) at the effluent weirs of a conical lamella settler can be predicted. The conical lamella settler was subjected to various constant flow rates (0,1 to 3 $m^3 \cdot h^{-1}$) which resulted in a change of the hydraulic retention time T of the flocculator according to Eq. 7:

$$T = \frac{V}{Q} \qquad (7)$$

where:

V - volume of the flocculation basin (m^3).

The root mean square velocity gradient G was also varied for a particular chosen flow rate. The residual turbidity of the effluent from the conical lamella settler was analysed after the clarifier had come to equilibrium. The clarifier performance is plotted, together with the theoretical predictions (Figs. 11 and 12). The figures show that the theoretical model provides a reasonable estimate of the residual turbidities that may be achieved in the clarifier.

Hydraulic residence times

Rebhun and Argaman (1965) have developed an equation which can be utilised to evaluate a basin's hydraulic characteristics. They showed that the decimal part of the fluid retained in a reactor for a duration longer than time t is given by:

$$1 - F(t) = e^{-\left[(1-p)(1-q)^{-1}\right]t/T - p(1-q)\Big]} \qquad (8)$$

where:

F(t) - fraction of fluid remaining in the reactor for a duration less than time t

T - nominal or theoretical retention time (T = V/Q), (s)

V - volume of the reactor (m^3)

Q - total flow rate through the reactor ($m^3 \cdot s^{-1}$)

p - fraction of the live volume exhibiting plug flow characteristics

l-p - fraction of the live volume exhibiting mixed flow characteristics

q - fraction of the total basin that is dead space

The basin volume fractions can be evaluated from tracer test curves as indicated in Fig. 13. Tracer tests were carried out on the clarifier for liquid/air interface overflow rates varying from v = 2 $m \cdot h^{-1}$ to v = 8 $m.h^{-1}$ and flocculator basin root mean square velocity gradients of G = 10·s^{-1} to G = 60·s^{-1}.

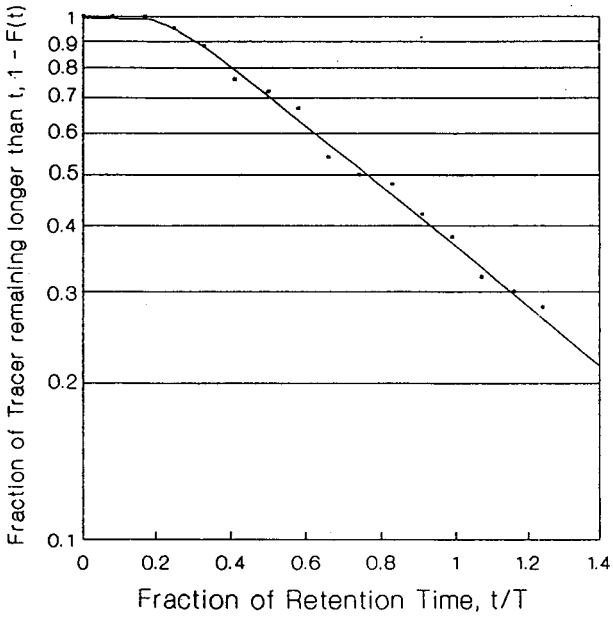

Figure 13
Tracer test curve

It was found that the dead space in the flocculator varied from a positive value of q 5% at G = 10·s^{-1} to a negative fraction of q = - 1,5% at G = 60·s^{-1}. At G = 30·s^{-1} the floc basin dead space was equal to zero. At the low mixing intensity of G = 10·s^{-1} the flocculator impeller was imparting insufficient power to the reactor volume to allow the flocculator to operate as a completely mixed flow reactor in series and therefore unutilised dead space persisted in the basin. At the higher mixing intensity of G = 60·s^{-1} negative dead space persisted, meaning that some back mixing was

occurring due to the pumping action of the impeller and that the flocculator was borrowing space from the settling basin. This variation in dead space means that the effective volume of the floc basin changes and consequently its residence time T is directly influenced. The fractional change of theoretical hydraulic retention time for the floc basin is illustrated in Fig. 14. If this variation is incorporated into the model describing the conical lamella settler performance, a revised residual turbidity prediction is obtained (Fig. 15). Figure 15 illustrates that the inclusion of an adjusted flocculator basin hydraulic retention time has a negligible effect on the clarifiers' performance, i.e. the effects due to short-circuiting through the flocculator may be ignored.

Another phenomenon highlighted by the tracer tests is that at low overflow rates of v = 2 m·h^{-1} dead space is created in the plate pack due to the pumping capacity of the axial flow impeller. This dead space exists at the bottom of the plate pack (Barthelme (1989)) and increases as G increases. The change in dead zone fraction results in a smaller utilisation of the number of plate cells. This is illustrated in Fig. 16. The theoretical plate cell utilisation at G = 0·s^{-1} is 9. The settling velocities (v_s) that result due to the revised number of plate spacings (n) at successive mixing intensities are graphically represented in Fig. 17. Substituting these adjusted settling velocities into the clarifier performance model does not result in any significant change in residual turbidity prediction (Fig. 18). The conical lamella settler therefore seems relatively insensitive to changes in the purification variables caused by its hydraulic characteristics. This phenomenon is also born out by other researchers, Zeevalkink and Brunsmann (1983).

Plate pack flocculation effect

Laminar fluid flow between the conical plates results in a parabolic velocity profile that flattens out from the inlet to the outlet of the plate cell. The average flow velocity also reduces from the inlet to the outlet of the conical plates and hence a two-dimensional point velocity gradient field is set up as illustrated in Fig. 19. The point velocity gradient is defined as the rate of change of velocity with distance (Camp and Stein, 1943) and for a conical plate cell is given by:

$$G_{(h_o,\, z)} = \left[\left[\frac{\partial u}{\partial h_o} \right]^2 + \left[\frac{\partial u}{\partial z} \right]^2 \right]^{1/2} \qquad (9)$$

where:

- u - local or point velocity in the laminar profile between two plates (m·s^{-1})
- h_o - cone radius between inlet and outlet, ie: $h \leq h_o \leq H$(m)
- z - plate spacing depth such that $0 \leq z \leq Z$ (m)

Barthelme (1989) has shown that the average root mean square velocity gradient created by the plate pack as a result of the shear stresses set up by the surface friction on the plates is given by:

$$G_2 = \frac{3Q}{\pi (H - h)\, n \cos\alpha} \left[\frac{1}{30Z} \left[\frac{1}{h} - \frac{1}{H} \right] + \frac{1}{3Z^3} \left[\ln \frac{H}{h} \right] \right] \qquad (10)$$

where:

- G_2 - average root mean square velocity of plate pack (s^{-1})
- n - number of plate spacings
- α - inclination angle of plates

Figure 20 shows how G_2 varies for the conical lamella settler. The figure indicates that the plate pack mixing is entirely hydraulic and in a similar way to the floc basin preceding it, may also contribute

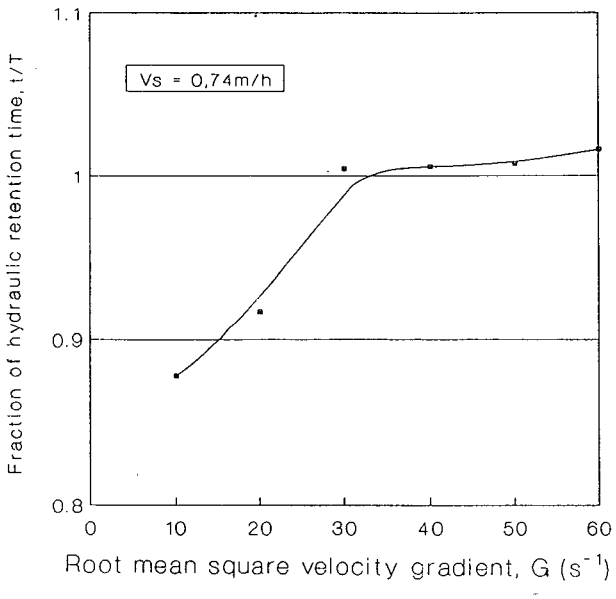

Figure 14
Fractional change of the flocculator hydraulic retention time with an increase in the mixing intensity

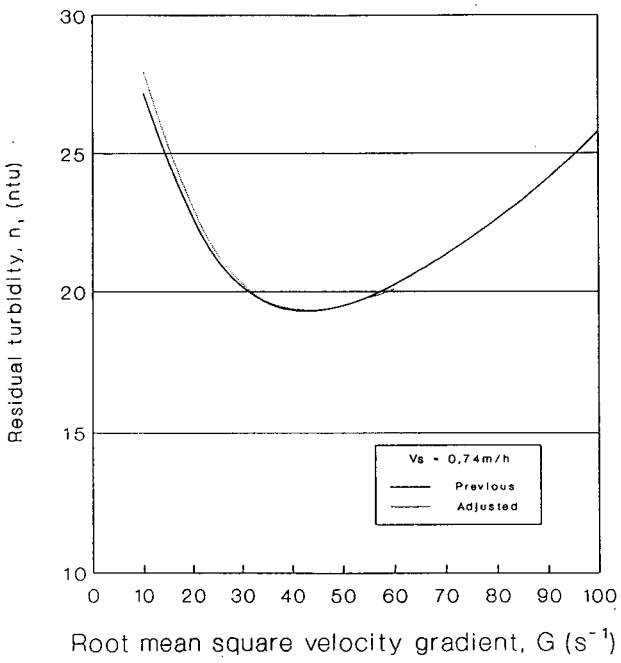

Figure 15
Clarifier performance with adjusted flocculator hydraulic retention time

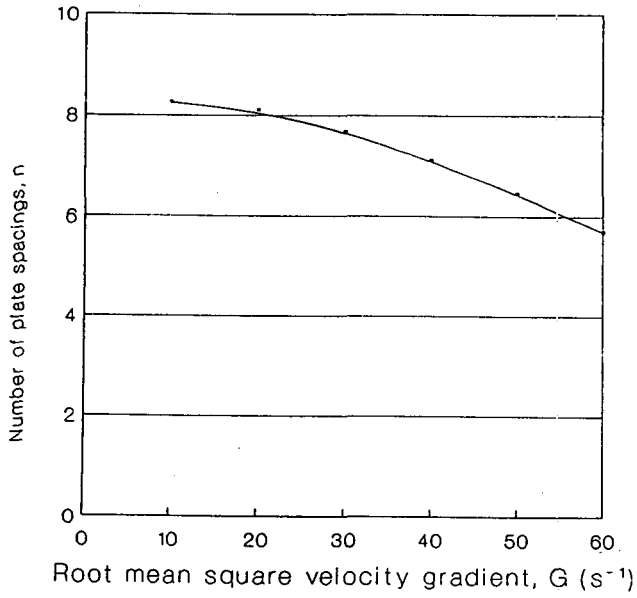

Figure 16
Plate cell utilisation at v = 2 m·h⁻¹

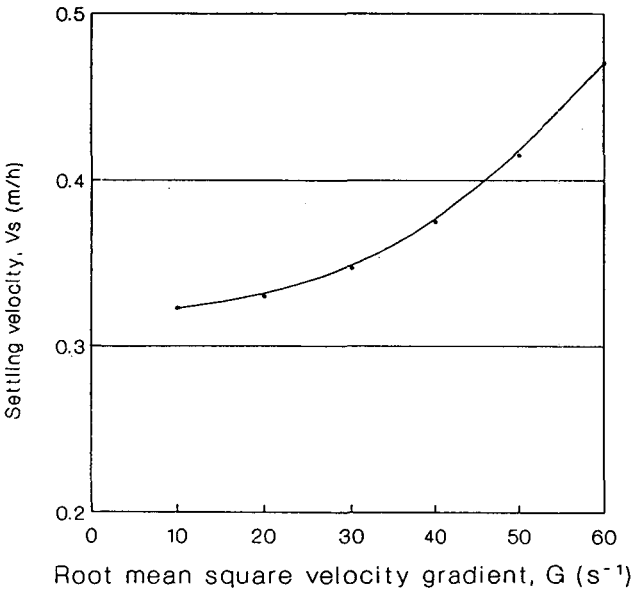

Figure 17
Actual settling velocities existing in the plate pack

to the flocculation of the effluent. What is required is some estimate of the magnitude of residual turbidity reduction brought about by the plate pack in the form of flocculation. Tracer tests conducted on the conical lamella settler have shown that the plate pack exhibits a 71% plug flow fraction. The plate pack may therefore be modelled as a plug flow reactor in series with the flocculation basin which exhibits completely mixed hydraulic characteristics. The above approach does not, however, take into account that the concentration of the flocs decreases along the plate length as settling takes place. Hence flocculation will not be constant between the plates but will decrease from the plate inlet to the outlet as progressively fewer flocs are present in the water to affect particle aggregation. Modelling the plate pack as a batch reactor will therefore only provide an upper limit to its flocculation efficiency. Using Eq. 1 to model the flocculation basin and Eq. 2 as representative of the plate pack, it can be shown that the combined maximum possible flocculation efficiency of the clarifier is given by:

$$\frac{n_o}{n_2} = \frac{(1 + k_A GT)\left[\frac{k_B}{k_A} G_2 + \left[1 - \frac{k_B}{k_A} G_2\right] e^{-k_A G_2 T_2}\right]^{-1}}{(1 + k_B G^2 T)} \quad (11)$$

where:

n_2 - residual turbidity at the end of the plate pack
T_2 - hydraulic retention time of the plate pack (s)

Figure 21 shows that for the conical lamella settler, the plate pack may contribute only approximately a 1 ntu reduction in residual turbidity due to its flocculation capacity. Therefore the flocculation basin contributes to the major portion of the flocculation and a lamella settler cannot function effectively without a flocculator since the plates do not provide adequate velocity gradients and retention times on their own.

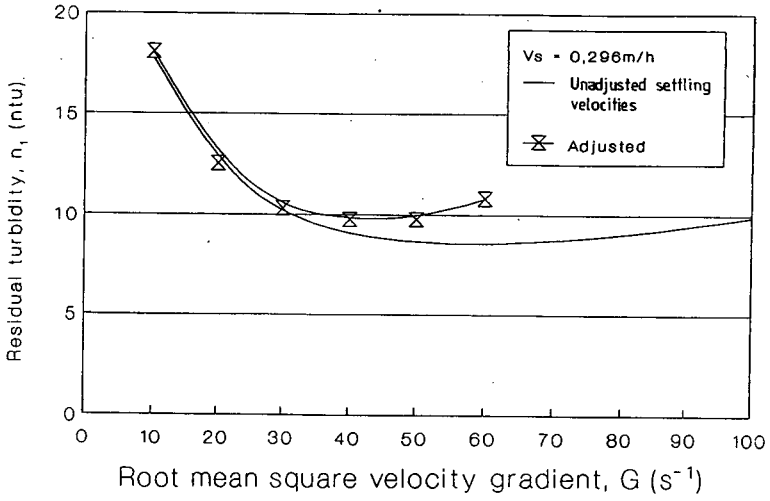

Figure 18
Theoretical clarifier performance with adjusted plate spacings

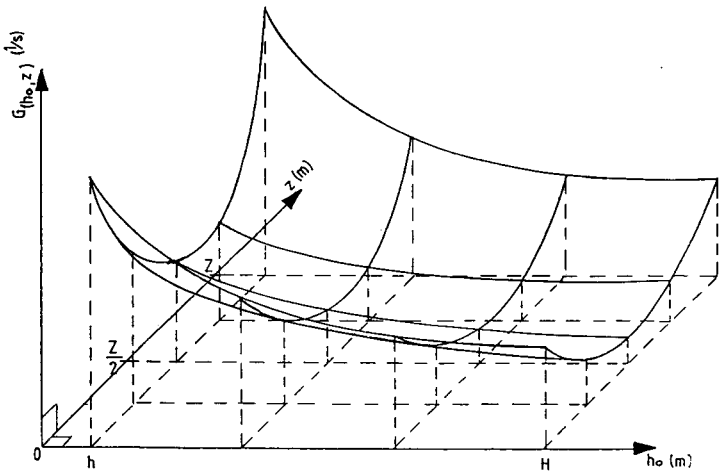

Figure 19
Point velocity gradient field between conical parallel plates

Clarifier optimisation

When an unconventional clarifier configuration is tested as a pilot plant it may be arbitrarily sized as to the residence times of the plate pack and the flocculation basin. The question that is now addressed is whether the clarifier with fixed holding tank dimensions can produce a clearer effluent if the number of plate cells (n) is increased to enhance settling. If the number of plate spacings is increased, then the volume of the flocculation tank is proportionally reduced since the new plate cells now occupy the volume that was formerly used for flocculation. However, not too many plate cells can be installed since eventually there will be insufficient volume available to flocculate the water properly. Hence there must be some point beyond which if the plate cells are increased the effluent quality will deteriorate. The above can also work in reverse, i.e. the number of plate spacings can be reduced to increase the floc basin volume. Again a point will be reached beyond which any advantages obtained by increasing the floc basin volume will be offset by the reduced sedimentation capacity. To obtain this optimum effluent clarity by physically changing the number of plates in the settler may be economically and physically impossible. Also such testing is time-consuming.

Alternatively, the minimum residual turbidity may be mathematically determined by writing the retention times of the floc basin and plate pack in terms of the number of plate spacings (n) and the root mean square velocity gradient (G) imparted by the flocculation basin impeller for a particular total flow rate Q (Barthelme, 1989). These retention times are then substituted back into Eq. 1. The residual turbidities n_i may be presented as a matrix with varying n and G for a particular Q (see Fig. 22). On closer scrutiny of the three-dimensional surface, it becomes clear that some residual turbidity values, in particular the negative ones, are nonsensical. This is because the optimum that the curves exhibit with G is very narrow and a slight increase in G results in a large change in n_i. This means that the conical lamella clarifier is unable to purify the raw water with fewer than 4 plates for this particular given situation.

The matrix also shows that as the number of plate cells increases from n = 4 to n = 9, the residual turbidity decreases for a constant G value. If the number of plate cells is increased above n = 9, then the residual turbidity increases. This increase in turbidity is brought about by the reduction in the flocculator volume which now becomes more critical than the increase in the sedimentation region. Therefore, for the particular Q chosen, n = 9 plate spacings will provide the clearest effluent from the clarifier. The matrix also shows that a maximum residual turbidity trend also exists in the rows. It shows that a maximum residual turbidity is obtained at $G = 60 \cdot s^{-1}$ and n = 9. Similarly, the optimum operating conditions of the clarifier can be obtained for the entire envisaged range of flow rates. The n and G values which produce the lowest residual turbidities from a bentonite suspension of 40 ntu are plotted in Fig. 23.

Figure 24 illustrates the minimum residual turbidities that are

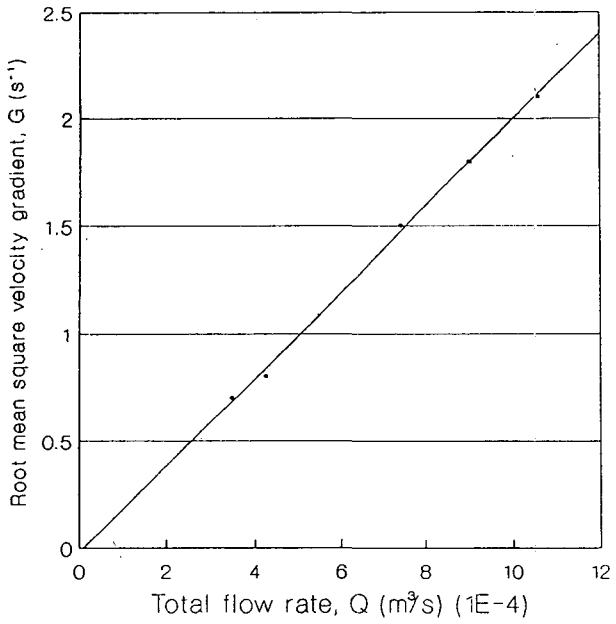

Figure 20
Root mean square velocity gradients in the plate pack

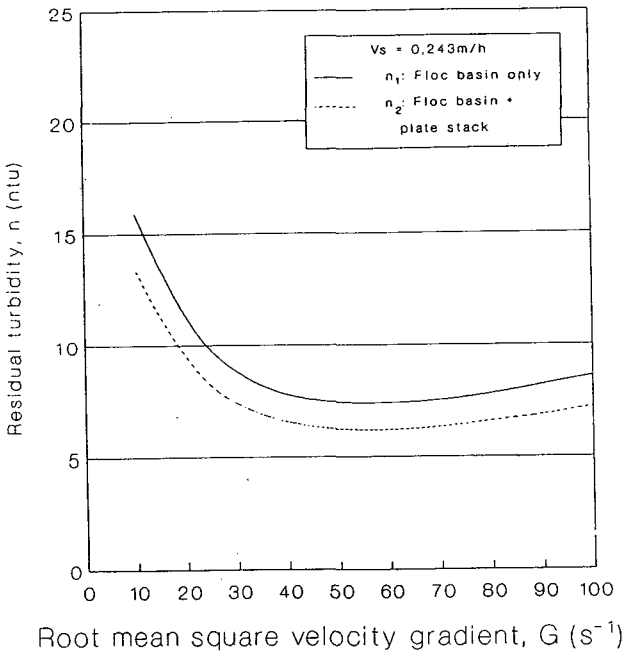

Figure 21
Clarifier performance

obtainable for the bentonite and kaolin suspensions if the number of plate spacings and flocculator basin mixing intensities are adjusted according to the optimums in Fig. 23. Figure 24 also highlights the fact that waters with different characteristics produce flocs with different settling characteristics.

Summary of conclusions

This study was aimed at developing a theory around the standard laboratory jar test for designing and operating full-scale continuous clarification unit processes. If the settling depth in the jar is the same as that of the clarifier (which is possible in plate settlers), then settling data may be applied directly to the continuous clarifier. The floc break-up rate and floc aggregation rate constants are statistically correlated to the floc settling velocities. The constants in the correlations are typical for the particular type of water. The model so developed may be utilised in obtaining a first estimate of the size and performance of a shallow depth sedimentation device.

The model and the laboratory jar test are also useful in evaluating the effect of the hydraulic characteristics on the clarification performance of a continuous process. It was shown that a lamella settler will not perform satisfactorily without a flocculation basin preceding the plate pack since the velocity gradients persisting between the plates are low and of too short a duration. The optimum operating conditions and clarifier configuration may be obtained through jar test modelling without having to make physical changes to pilot plants which may be expensive and time-consuming.

$Q = 4{,}0 \times 10^{-4}\ m^3 \cdot s^{-1}$

G(/s) / n	10	20	30	40	50	60	70	80	90	100
1	-105	-197	-291	-358	-480	-575	-669	-764	-859	-954
2	-26	-26	-36	-39	-46	-54	-62	-71	-79	-87
3	35	44	57	75	94	114	135	157	180	203
4	12,1	9,4	9,4	10,3	11,5	12,9	14,5	16,1	17,8	19,5
5	8,7	6,0	5,5	5,6	6,0	6,5	7,1	7,8	8,5	9,2
6	7,6	5,0	4,3	4,1	4,3	4,5	4,8	5,2	5,6	6,1
7	7,3	4,6	3,8	3,6	3,6	3,7	3,9	4,1	4,4	4,7
8	7,4	4,6	3,7	3,4	3,3	3,3	3,4	3,5	3,7	4,0
9	7,9	4,9	3,8	3,4	3,2	(3,2)	3,2	3,3	3,4	3,6
10	8,9	5,5	4,2	3,6	3,3	3,2	3,2	3,2	3,3	3,4
11	10,2	6,5	4,9	4,2	3,8	3,6	3,4	3,4	3,4	3,5

Figure 22
Residual turbidity matrix

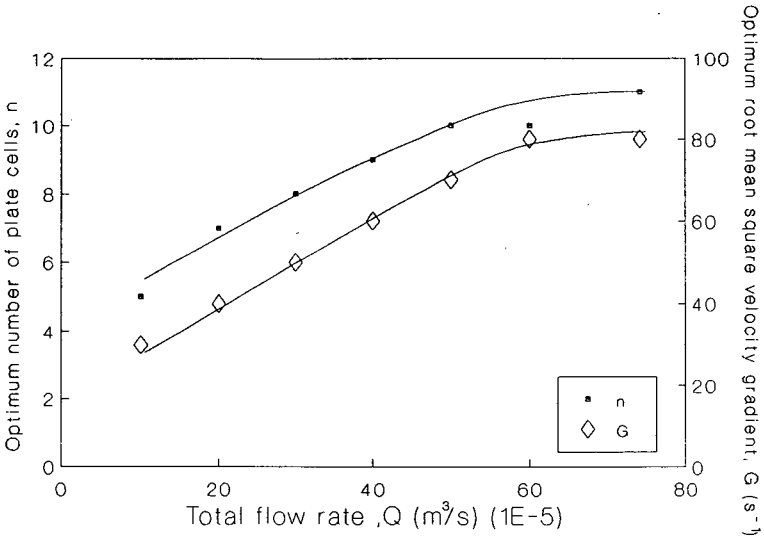

Figure 23
Optimum operating conditions

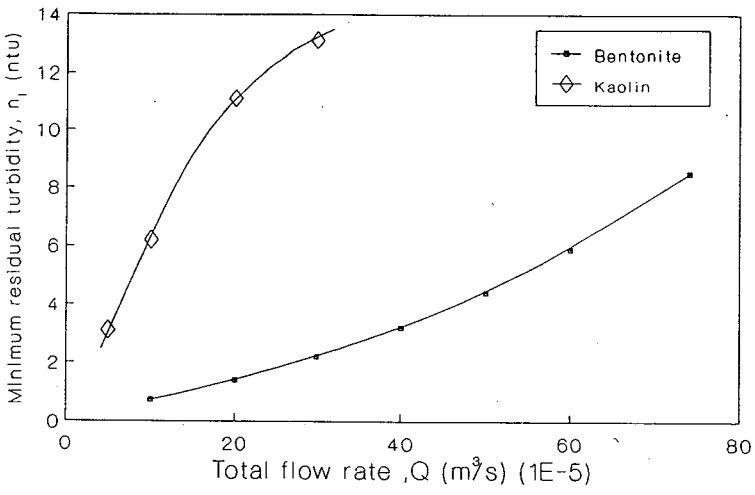

Figure 24
Minimum residual turbidites for different clay suspensions

Acknowledgements

The results presented in this paper are part of a larger study undertaken at the University of the Witwatersrand, Department of Civil Engineering, Johannesburg, South Africa, in partial fulfilment of the Ph. D degree.

References

ANDREU-VILLEGAS, R and LETTERMAN, R D (1976) Optimising flocculator power input. *J. Env. Eng. Dir. ASCE* **102** (EE2) 251.

ARGAMAN, Y A (1971) Pilot plant studies of flocculation. *J. AWWA* **63** 775.

ARGAMAN, Y A and KAUFMAN, W (1970) Turbulence and flocculation. *J. SED ASCE* 223.

BARTHELME, S H (1989) Design of Conical Lamella Settlers with the Aid of Jar Tests. Ph.D. thesis, University of the Witwatersrand, Johannesburg, SA.

BATES, R L, FONDY, P L and CORPSTEIN, R R (1963) An examination of some geometric parameters of impeller power. *I&EC Process Design and Development* **2** (4) 310.

BENEFIELD, L D, JUDKINS, J F and WEAND, B L (1982) *Process chemistry of Water and Wastewater Treatment.* Prentice Hall Inc, Englewood Cliffs, NJ, USA.

BRATBY, J, MILLER, M W and MARAIS, G (1977) Design of flocculation systems from batch test data. *Water SA* **3** (4) 172.

CAMP, T R and STEIN, P C (1943) Velocity gradients and internal work in fluid motion. *J. of the Boston Soc. of Civil Eng.* 219.

CLEASBY, J L (1984) Is velocity gradient a valid turbulent flocculation parameter? *J. Env. Eng. Div. ASCE* **110** (5) 875.

HUDSON, H E (1981) *Water Clarification Processes. Practical Design and Evaluation.* Van Nostrand Renhold Company, New York.

JANSSENS, J G and BEUKENS, A (1987) Theoretical analysis and practical application of the kinetic model of flocculation in the interpretation of the jar test. *Aqua* **2** 99.

LAI, R J, HUDSON, H E and SINGLEY, J E (1975) Velocity gradient calibration of jar test equipment. *J. AWWA* **67** 553.

LEENTVAAR, J and YWEMA, TSJ (1980) Some dimensionless parameters of impeller power in coagulation - Flocculation processes. *Water Res.* **14** 135.

REBHUN, M and ARGAMAN, Y (1965) Evaluation and hydraulic efficiency of sedimentation basins. *J. SED ASCE* 37.

YAO, K M (1970) Theoretical study of high rate sedimentation. *J. WPCF* **42** 218.

ZEEVALKINK, J A and BRUNSMANN, J J (1983) Oil removal from water in parallel plate gravity-type separators. *Water Res.* **17** (4) 365.